Synthesis, Characterization, Molecular Modeling, and Biological Evaluation of 1,2,4-Triazole-pyridine Hybrids as Potential Antimicrobial Agents

J. Ahirwar,[a]* D. Ahirwar,[a] S. Lanjhiyana,[a] A. K. Jha,[b] D. Dewangan,[c] and H. Badwaik[c]

[a]School of Pharmacy, Chouksey Engineering College, Bilaspur, Chhattisgarh, India
[b]Shri Shankaracharya Institute of Pharmaceutical Science, Bhilai, Chhattisgarh, India
[c]Rungta College of Pharmaceutical Sciences and Research, Bhilai, Chhattisgarh, India
*E-mail: jyoti_ah@yahoo.com
Received March 14, 2018
DOI 10.1002/jhet.3319
Published online 00 Month 2018 in Wiley Online Library (wileyonlinelibrary.com).

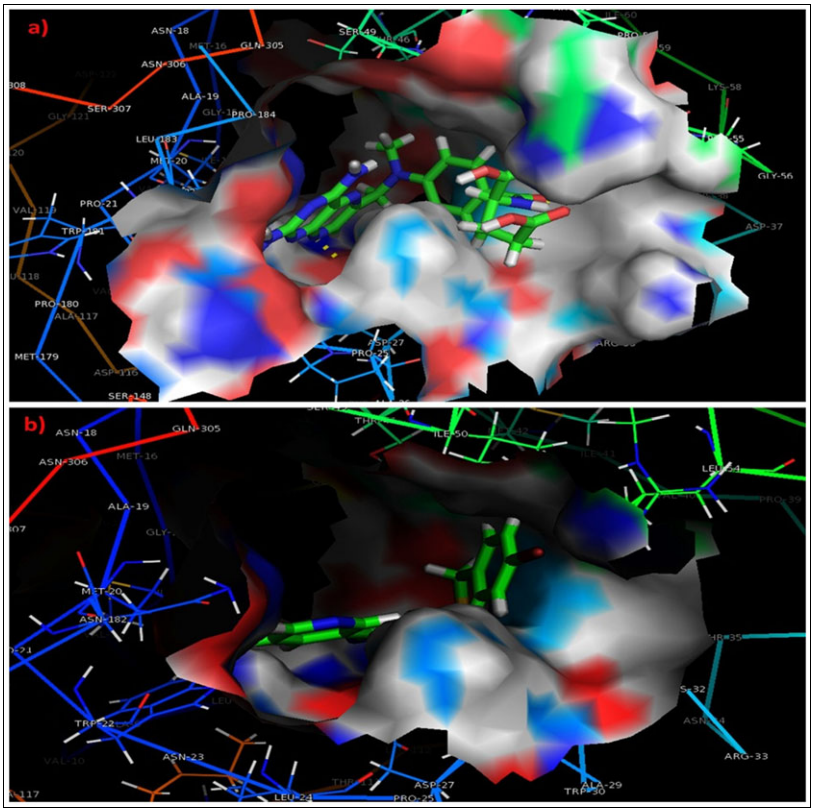

A novel 1,2,4-triazole-pyridine hybrid derivatives were synthesized by the reaction of nicotinohydrazide with carbon disulfide to yield potassium-3-pyridyl-dithiocarbazate (**I**). This was further cyclized with ammonia solution to yield 5-mercapto-substituted 1,2,4-triazole-pyridine hybrid (**II**). This was finally reacted with different substituted benzyl derivatives to produce 1,2,4-triazole-pyridine hybrid derivatives (**III**). The purity of the derivatives was confirmed by thin-layer chromatography and melting point. Structure of these derivatives was set up by determining its infrared spectroscopy, nuclear magnetic resonance spectroscopy, and mass spectroscopy. Further, the synthesized derivatives were evaluated for their in vitro antimicrobial activity against the three Gram-negative bacteria (*Escherichia coli*, *Pseudomonas aeruginosa*, and *Acinetbacter baumannii*), three Gram-positive bacteria (*Staphylococcus aureus*, *Streptococcus pyogenes*, and *Enterococcus faecalis*), and two fungus (*Aspergillus clavatus* and *Candida albicans*). Minimal inhibitory concentration was also determined against same microorganism. Out of all synthesized derivatives, two derivatives, that is, 3-(5-(2-bromobenzylthio)-4*H*-1,2,4-triazol-3-yl)pyridine and 3-(5-(2,4-dibromobenzylthio)-4*H*-1,2,4-triazol-3-yl)pyridine showing more potent antibacterial activity.

Docking studies were performed by using Argus lab, and all the derivatives exhibited good docking scores between −10.5369 and −11.8477 kcal/mol and were better as compared with standard drug methotrexate against a dihydrofolate reductase protein fragment from *E. coli* and *Lactobacillus* (4DFR). Among all compounds, **4h** has shown the maximum docking score and found in agreement to in vitro antimicrobial studies.

INTRODUCTION

The emerging infectious diseases and the increasing number of multidrug resistant microbial pathogens are the main challenges behind the treatment of infectious diseases. In spite of a wide range of antimicrobial drugs with different mechanisms of action used to treat microbial infections either alone or in combination and also the existence many compounds in different phases of clinical trials, microbial infections have been becoming a worldwide problem. An increase in mortality might be due to the emergence of antimicrobial resistance [1–3]. The toxic side effects and the increasing chances of microbial resistance are the problems with clinically used drugs that are often dose-limiting [4,5]. Moreover, the long-term use of several drugs to treat microbial infections may cause serious health problems, especially in patients with impaired liver or kidney functions.

To search and synthesize of combinational chemotherapeutic drugs with different mechanisms of action and with low side effects constitute an important part of the methods that aims to overcome the antimicrobial resistance. Beside the development of completely new agents possessing chemical characteristics that clearly differ from those of existing ones, there is another approach containing to combine two or more pharmacophores into a single molecule [6–8]. Therefore, more than one pharmacophores (with a different mode of action) containing a hybrid molecule could be beneficial for the treatment of microbial infections. These merged pharmacophores may be addressing the active site of different targets and offer the possibility to overcome drug resistance. In addition, this approach can also reduce unwanted side effects [9–11].

Among the broad range of heterocyclic that is being explored for expansion of new components in the field of medicinal chemistry, 1,2,4-triazole-pyridine hybrids and their fused heterocyclic derivatives have acknowledged significant consideration due to their synthetic and effective biological importance [12–19]. The triazole is an attractive bridge group, which could connect two pharmacophores to produce novel bifunctional molecules, while it is almost impossible to be hydrolyzed, oxidized, or reduced.

Based on these literature data and the features described previously, we have created a small library of 1,2,4-triazole-pyridine hybrid derivatives as per Figure 1. All the synthesized compounds were screened for antimicrobial activity and compared with the commercial antibiotic. The antimicrobial activity of derivatives was assessed on three Gram-negative bacteria (*Escherichia coli*, *Pseudomonas aeruginosa*, and *Acinetbacter baumannii*), three Gram-positive bacteria (*Staphylococcus aureus*, *Streptococcus pyogenes*, and *Enterococcus faecalis*) by using plate hole diffusion method using methotrixate as a standard drug, and two fungus (*Aspergillus clavatus* and *Candida albicans*) by modified microdilution method using fluconazole as a standard drug. Dihydrofolate reductase (DHFR) inhibition has long been identified as an important target for the development of chemotherapeutic agents against bacterial and parasitic infections. This made the DHFR as an ideal target for rational and efficient drug design.

Several studies showed that triazole analogs can be used as potential DHFR inhibitors [20,21]. It is a well-known fact that DHFR is a key enzyme in the folate metabolism. DHFR enzyme inhibition results in depletion of intracellular reduced folates necessary for one-carbon

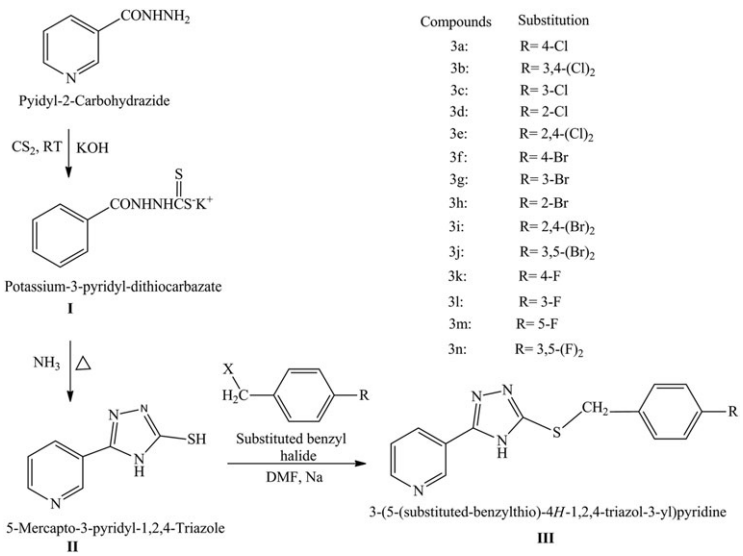

Figure 1. Scheme for synthesis of 1,2,4-triazole-pyridine hybrid derivatives.

transfer reactions which, in turn, are important for the biosynthesis of thymidylate, purine nucleotides, methionine, and many other compounds necessary for RNA, DNA, and protein synthesis [22]. Molecular docking study was performed to interpret the comparative differences in the binding interactions of the synthesized and commercial antibiotic at the molecular level as inhibitors of DHFR as an antimicrobial agent.

EXPERIMENTAL

An open capillary method was adopted to determine the melting points, and the purity of compounds was checked by thin-layer chromatography (TLC) [23,24]. Fourier transform infrared spectra (KBR, cm^{-1}) were recorded on Perkins Elmer Infrared-283 Fourier transform infrared; ^{1}H NMR (DMSO) and ^{13}C NMR were on a Bruker 300 MHz spectrometer using tetramethylsilane as an internal reference; and the mass spectrometry (MS) was recorded on Aapi 3000 LC–MS.

The synthesized compounds **3a**–**3n** were examined for their in vitro antimicrobial activity against the three Gram-negative bacteria [*E. coli* (MTCC 443), *P. aeruginosa* (MTCC424), and *A. baumannii* (MTCC 1425)], three Gram-positive bacteria [*S. aureus* (MTCC 96), *S. pyogenes* (MTCC 442), and *E. faecalis* (MTCC 439)] by using plate hole diffusion method [25–27], and two fungus [*A. clavatus* (MTCC 1323) and *C. albicans* (MTCC 227)] by modified microdilution method [28]. Zone of inhibition of all derivatives was determined and compared with standard methotrexate and fluconazole, which were used as reference drug. The minimal inhibitory concentration study was performed by microdilution susceptibility method [22].

Synthesis of potassium-3-pyridyl-dithiocarbazate (I) [29]. A solution of 8.4 g (0.15 M) of potassium hydroxide (CAS 1310-58-3), 200 mL of absolute ethanol (CAS 64-17-5), and 13.7 g (0.10 M) of pyridyl-2-carbohydrazide (CAS 1452-63-7) was treated to the addition of 11.4 g (0.15 M) of carbon disulfide (CAS 75-15-0). The mixture was diluted with 150 mL of absolute ethanol and agitated for 12–16 h. It was then diluted with 200 mL of dry ether and dried at 65°C. The salts, prepared as described above were utilized in the next step without further purification.

Synthesis of 5-mercapto-3-pyridyl-1,2,4-triazole (II) [30]. A suspension of **I** (24 g, 0.096 M), 95% ammonia (CAS 7664-41-7) 20 mL (0.864 M), and water 40 mL was refluxed with stirring for 3 to 4 h. The color of this reaction mixture changed to yellow, hydrogen sulfide was evolved, and a homogeneous solution resulted. A white solid was precipitated by dilution with cold water (100 mL) and acidify with concentrated HCL, filtered and washed with cold water and recrystallized.

Synthesis of 3-benzylthio-5-pyridin-3-yl,1,2,4-triazole (III). A mixture of **II** (0.006 M), (0.69 g, 6 M) in dry *N*,*N*-dimethylformamide (CAS 68-12-2) (3 mL) was added to a solution of sodium (0.14 g, 6 M) in dry methanol (CAS 67-56-1) (2 mL). After 10 min of stirring at room temperature, benzyl halide (6 M) was added. The resultant suspension was stirred with $CaCl_2$ guard tube at room temperature 1–23 h. The completion of the reaction was confirmed by TLC and then resultant solution was poured in crushed ice.

Molecular docking study. Molecular docking study was performed using Argus Lab 4.0 docking software to find the mode of corresponding interactions of the test compound with the target. Protein structure of DHFR from *E. Coli* and *Lactobacillus* (4DFR) was obtained

Table 1

Docking parameters used in Argus Lab 4.0.1.

Compound ID(s)	Constant term	vdW coefficient	H-bond coefficient neutral-neutral	Rotors coefficient	Hydrophobic coefficient
3a	2.783	−0.00096	0.38	−0.1	0.0373
3b	2.783	−0.00096	0.38	−0.1	0.0373
3c	2.783	−0.00096	0.38	−0.1	0.0373
3d	2.783	−0.00096	0.38	−0.1	0.0373
3e	2.783	−0.00096	0.38	−0.1	0.0373
3f	2.783	−0.00096	0.38	−0.1	0.0373
3g	2.783	−0.00096	0.38	−0.1	0.0373
3h	2.783	−0.00096	0.38	−0.1	0.0373
3i	2.783	−0.00096	0.38	−0.1	0.0373
3j	2.783	−0.00096	0.38	−0.1	0.0373
3k	2.783	−0.00096	0.38	−0.1	0.0373
3l	2.783	−0.00096	0.38	−0.1	0.0373
3m	2.783	−0.00096	0.38	−0.1	0.0373
3n	2.783	−0.00096	0.38	−0.1	0.0373

Grid parameters: spacing 0.375 Å and grid size 80X Å, 80Y Å, and 80Z Å.

from the Protein Data Bank. The three-dimensional structure of the investigated molecules in their natural form was constructed using Chem Draw Ultra 10.0. In the Argus Lab 4.0 program, lowest energy conformer of each of the new analogs was docked into DHFR binding domain. In the present study, protein–ligand interaction was determined by using Pymol 1.3 software.

RESULTS AND DISCUSSION

In the present study, for the first time, we have reported the antimicrobial evaluation of synthesized 3-(5-(substituted-benzylthio)-4*H*-1,2,4-triazol-3-yl)pyridine derivatives. The synthesized 1,2,4-triazole derivatives were subjected to confirmation of physical and analytical parameters by using techniques like combustion analysis, TLC, IR, NMR, and MS. Finally, these compounds were screened for in vitro antibacterial and antifungal activity.

The synthetic way used to produce different 1,2,4-triazole derivatives is outlined in Figure 1. Total 14 different 1,2,4-triazole derivatives were prepared by treating 5-mercapto-3-pyridyl-1,2,4-triazole with differently substituted benzyl halides. Docking parameters used in Argus lab 4.0.1 were mentioned in Table 1. Properties of ligands on the basis of their molecular structure were mentioned in Table 2. Chemical properties of ligands were mentioned in Table 3. Docking results of ligands and standard drug against DHFR (4DFR) were mentioned in Table 4. Chemical structure, melting point, and other physical data were mentioned in Table 5. Data of combustion analysis was mentioned in Table 6.

Table 2

Properties of ligands on the basis of their molecular structure.

Compound ID(s)	Molecular parameters[a]							
	Stretch	Bend	Stretch-bend	Torsion	Non-1,4 VDW	1,4 VDW	Dipole/dipole	Total energy (kcal/mol)
3a	0.7730	12.5043	−0.0414	−9.4392	−2.2321	13.8876	−2.8071	12.6451
3b	0.9027	12.8240	−0.0112	−11.0387	−2.3892	15.1217	−0.2819	15.1273
3c	0.7791	12.4803	−0.0430	−9.4399	−2.2626	13.9150	−2.8233	12.6056
3d	0.9073	12.8141	−0.0289	−9.1133	−1.7173	14.1282	−3.0422	13.9479
3e	0.9365	12.8492	−0.0198	−9.1127	−1.8841	14.6221	−2.3606	15.0306
3f	0.7813	12.5493	−0.0317	−9.4394	−2.2782	14.0425	−2.8039	12.8199
3g	0.7882	12.5204	−0.0331	−9.4401	−2.3236	14.0762	−2.8186	12.7695
3h	0.9604	13.0036	−0.0088	−9.4293	−1.6553	14.3367	−2.9906	14.2167
3i	1.0024	13.0722	0.0111	−9.4316	−1.8956	15.0143	−2.3989	15.3740
3j	0.8353	12.5706	−0.0136	−9.4381	−2.6184	14.7617	−2.2393	13.8581
3k	0.7534	12.4597	−0.0551	−9.4390	−2.1162	13.3324	−2.8105	12.1247
3l	0.7541	12.4649	−0.0559	−9.4394	−2.1201	13.3347	−2.8284	12.1099
3m	0.7872	12.5149	−0.0590	−9.4402	−1.9861	13.4803	−3.1684	12.1288
3n	0.7927	12.5290	−0.0637	−9.4390	−2.0087	13.3673	−2.3683	12.8094

[a]Data generated using ChemBioDraw 13 software after MM2 energy minimization.

Table 3

Chemical properties of ligands.

Compound ID(s)	Molecular formula	Molecular mass (g/mol)	CLogP values*	CMR	Gibbs energy: [kJ/mol]
3a	$C_{14}H_{11}ClN_4S$	302	2.88	8.26	782.77
3b	$C_{14}H_{10}Cl_2N_4S$	337	3.47	8.76	761.21
3c	$C_{14}H_{11}ClN_4S$	302	2.88	8.26	782.77
3d	$C_{14}H_{11}ClN_4S$	302	2.88	8.26	782.77
3e	$C_{14}H_{10}Cl_2N_4S$	337	3.47	8.76	761.21
3f	$C_{14}H_{11}BrN_4S$	347	3.03	8.55	809.02
3g	$C_{14}H_{11}BrN_4S$	347	3.03	8.55	809.02
3h	$C_{14}H_{11}BrN_4S$	347	3.03	8.55	809.02
3i	$C_{14}H_{10}Br_2N_4S$	426	3.89	9.33	813.71
3j	$C_{14}H_{10}Br_2N_4S$	426	3.89	9.33	813.71
3k	$C_{14}H_{11}FN_4S$	286	2.31	7.89	599.89
3l	$C_{14}H_{11}FN_4S$	286	2.31	7.89	599.89
3m	$C_{14}H_{11}FN_4S$	286	2.31	7.89	599.89
3n	$C_{14}H_{10}F_2N_4S$	304	2.45	7.80	395.45

*Data generated using ChemBioDraw 13 software.

Table 4

Docking results of ligands and standard drug against DHFR (4DFR).

Compound ID(s)	Binding energy (kcal/mol)	No. of hydrogen bonds	Bond length of H-bonds in Å	H-bond with receptor residue	Enzyme's binding site residue
3a	−11.016	1	2.695	211 ARG	188 ALA (ALPHA HELIX), 211 ARG (BETA STRAND), 216 ARG (COIL), 209 ILE (ALPHA HELIX), 253 ILE (COIL), 187 LEU (ALPHA HELIX), 213 LEU (BETA STRAND), 197 LYS (ALPHA HELIX), 201 MET (BETA STRAND), 190 PHE (ALPHA HELIX), 205 THR (ALPHA HELIX)
3b	−11.2976	2	2.633	300 HIS	185 ALA (ALPHA HELIX), 188 ALA (ALPHA HELIX), 298 GLU (BETA STRAND), 300 HIS (BETA STRAND), 314 ILE (BETA STRAND), 319 LYS (BETA STRAND), 296 PHE (BETA STRAND), 312 PHE (BETA STRAND), 189 TRP (ALPHA HELIX), 310 TYR (BETA STRAND)
			2.825	300 HIS	
3c	−11.8369	1	2.467	181 TRP	165 ALA (BETA STAND), 166 ALA (BETA STAND), 186 ASP (ALPHA HELIX), 164 ILE (BETA STRAND), 173 ILE (COIL), 209 ILE (ALPHA HELIX), 253 ILE (COIL), 187 LEU (ALPHA HELIX), 213 LEU (BETA STRAND), 179 MET (COIL), 190 PHE (ALPHA HELIX), 205 THR (ALPHA HELIX), 181 TRP (COIL), 259 TYR (ALPHA HELIX)
3d	−11.6663	2	2.989	94 ILE	6 ALA (BETA STRAND), 7 ALA (BETA STRAND), 57 ARG (BETA STRAND), 15 GLY (COIL), 95 GLY (COIL), 96 GLY (COIL), 97 GLY (COIL), 14 ILE (COIL), 50 ILE (ALPHA HELIX), 94 ILE (COIL), 28 LEU (ALPHA HELIX), 54 LEU (BETA STRAND), 31 PHE (ALPHA HELIX), 46 THR (ALPHA HELIX), 100 TYR (ALPHA HELIX)
			2.999	46 THR	
3e	−11.3277	2	2.553	211 ARG	188 ALA (ALPHA HELIX), 211 ARG (BETA STRAND), 216 ARG (COIL), 209 ILE (ALPHA HELIX), 253 ILE (COIL), 187 LEU (ALPHA HELIX), 213 LEU (BETA STRAND), 197 LYS (ALPHA HELIX), 201 MET (BETA STRAND), 190 PHE (ALPHA HELIX), 214 PRO (BETA STRAND), 205 THR (ALPHA HELIX)
			2.995	211 ARG	
3f	−10.6901	1	2.814	7 ALA	6 ALA (BETA STRAND), 7 ALA (BETA STRAND), 27 ASP (ALPHA HELIX), 5 ILE (BETA STRAND), 50 ILE (ALPHA HELIX), 94 ILE (COIL), 28 LEU (ALPHA HELIX), 54 LEU (BETA STRAND), 20 MET (COIL), 31 PHE (ALPHA HELIX), 46 THR (ALPHA HELIX), 22 TRP (COIL), 100 TYR (ALPHA HELIX), 182 ASN (COIL)
3g	−11.1236	0			6 ALA (BETA STRAND), 7 ALA (BETA STRAND), 57 ARG (BETA STRAND), 15 GLY (COIL), 95 GLY (COIL), 96 GLY (COIL), 97 GLY (COIL), 14 ILE (COIL), 50 ILE (ALPHA HELIX), 94 ILE (COIL), 28 LEU (ALPHA HELIX), 54 LEU (BETA STRAND), 31 PHE (ALPHA HELIX), 46 THR (ALPHA HELIX), 100 TYR (ALPHA HELIX)
3h	−11.8477	2	2.93	94 ILE	6 ALA (BETA STRAND), 7 ALA (BETA STRAND), 57 ARG (BETA STRAND), 15 GLY

(*Continues*)

Table 4

(*Continued*)

Compound ID(s)	Binding energy (kcal/mol)	No. of hydrogen bonds	Bond length of H-bonds in Å	H-bond with receptor residue	Enzyme's binding site residue
					(COIL), 95 GLY (COIL), 96 GLY (COIL), 97 GLY (COIL), 14 ILE (COIL), 50 ILE (ALPHA HELIX), 94 ILE (COIL), 28 LEU (ALPHA HELIX), 54 LEU (BETA STRAND), 20 MET (COIL), 31 PHE (ALPHA HELIX), 46 THR (ALPHA HELIX), 100 TYR (ALPHA HELIX)
			2.997	46 THR	
3i	−11.251	1	2.929	100 TYR	6 ALA (BETA STRAND), 7 ALA (BETA STRAND), 27 ASP (ALPHA HELIX), 5 ILE (BETA STRAND), 50 ILE (ALPHA HELIX), 94 ILE (COIL), 8 LEU (BETA STRAND), 28 LEU (ALPHA HELIX), 54 LEU (BETA STRAND), 20 MET (COIL), 31 PHE (ALPHA HELIX), 46 THR (ALPHA HELIX), 22 TRP (COIL), 100 TYR (ALPHA HELIX), 13 VAL (COIL)
3j	−10.7919	3	2.486	216 ARG	211 ARG (BETA STRAND), 216 ARG (COIL), 209 ILE (ALPHA HELIX), 253 ILE (COIL), 187 LEU (ALPHA HELIX), 213 LUC (BETA STRAND), 191 LYS (ALPHA HELIX), 201 MET (BETA STRAND), 190 PHE (ALPHA HELIX), 214 PRO (BETA STRAND), 205 THR (ALPHA HELIX)
			2.562	216 ARG	
			2.159	216 ARG	
3k	−10.6243	2	2.734	166 ALA	165 ALA (BETA STAND), 166 ALA (BETA STAND), 174 GLA (COIL), 164 I;LE (BETA STRAND), 173 ILE (COIL), 209 ILE (ALPHA HELIX), 253 ILE (COIL), 187 ILU (ALPHA HELIX), 213 LEU (BETA STRAND), 175 MET (COIL), 179 MET (COIL), 190 PHE (ALPHA HELIX), 205 THR (ALPHA HELIX), 181 TRP (COIL), 259 TYR (ALPHA HELIX)
			2.895	166 ALA	
3l	−11.0509	2	2.982	100 TYR	6 ALA (BETA STRAND), 7 ALA (BETA STRAND), 57 ARG (BETA STRAND), 15 GLY (COIL), 95 GLY (COIL), 96 GLY (COIL), 97 GLY (COIL), 5 ILE (BETA STRAND), 14 ILE (COIL), 50 ILE (ALPHA HELIX), 94 ILE (COIL), 28 LEU (ALPHA HELIX), 54 LEU (BETA STRAND), 31 PHE (ALPHA HELIX), 46 THR (ALPHA HELIX), 100 TYR (ALPHA HELIX)
			2.993	46 THR	
3m	−10.7385	1	2.999	46 THR	6 ALA (BETA STRAND), 7 ALA (BETA STRAND), 57 ARG (BETA STRAND), 15 GLY (COIL), 95 GLY (COIL), 96 GLY (COIL), 97 GLY (COIL), 5 ILE (BETA STRAND), 14 ILE (COIL), 50 ILE (ALPHA HELIX), 94 ILE (COIL), 28 LEU (ALPHA HELIX), 54 LEU (BETA STRAND), 31 PHE (ALPHA HELIX), 46 THR (ALPHA HELIX), 100 TYR (ALPHA HELIX)
3n	−10.5369	1	2.622	211 ARG	188 ALA (ALPHA HELIX), 211 ARG (BETA STRAND), 216 ARG (COIL), 209 ILE (ALPHA HELIX), 253 ILE (COIL), 187 LEU (ALPHA HELIX), 213 LEU (BETA STRAND), 191 LYS (ALPHA HELIX), 201 MET (BETA STRAND), 190 PHE (ALPHA HELIX), 214 PRO (BETA STRAND), 205 THR (ALPHA HELIX)

(*Continues*)

Table 4

(*Continued*)

Compound ID(s)	Binding energy (kcal/mol)	No. of hydrogen bonds	Bond length of H-bonds in Å	H-bond with receptor residue	Enzyme's binding site residue
Mithotrixate	−10.0287	4	1.847	52 ARG	7 ALA (BETA STRAND), 52 ARG (BETA STRAND), 57 ARG (BETA STRAND), 23 ASN (COIL), 27 ASP (ALPHA HELIX), 50 ILE (ALPHA HELIX), 94 ILE (COIL), 24 LEU (COIL), 28 LEU (ALPHA HELIX), 54 LEU (BETA STRAND), 32 LYS (ALPHA HELIX), 31 PHE (ALPHA HELIX), 46 THR (ALPHA HELIX), 22 TRP (COIL), 182 ASN (COIL)
			2.339	52 ARG	
			2.679	182 ASN	
			2.8539	22 TRP	

Grid parameters (Argus Lab.): spacing 0.375 Å and grid size 80X Å, 80Y Å, and 80Z Å.

Table 5

Characterization data of synthesized 1,2,4-triazole derivatives.

Compounds	R_1	Molecular formula	Molecular weight	Melting point (°C)	Appearance	Retention factor	Solubility	% yield (*w*/w)	λ max (nm)	Chemical name
3a	4-Cl	$C_{14}H_{11}ClN_4S$	302	207	White solid	0.72	Ethanol	73.73	345	3-(5-(4-chlorobenzylthio)-4*H*-1,2,4-triazol-3-yl)pyridine
3b	3,4-$(Cl)_2$	$C_{14}H_{10}Cl_2N_4S$	337	250	Creamy white solid	0.86	DMF	66.82	350	3-(5-(3,4-dichlorobenzylthio)-4*H*-1,2,4-triazol-3-yl)pyridine
3c	3-Cl	$C_{14}H_{11}ClN_4S$	302	207	Light brown solid	0.73	Ethanol	70	345	3-(5-(3-chlorobenzylthio)-4*H*-1,2,4-triazol-3-yl)pyridine
3d	2-Cl	$C_{14}H_{11}ClN_4S$	302	207	Brown solid	0.72	Ethanol	73	346	3-(5-(2-chlorobenzylthio)-4*H*-1,2,4-triazol-3-yl)pyridine
3e	2,4-$(Cl)_2$	$C_{14}H_{10}Cl_2N_4S$	337	250	Yellow solid	0.85	Ethanol	66.19	352	3-(5-(2,4-dichlorobenzylthio)-4*H*-1,2,4-triazol-3-yl)pyridine
3f	4-Br	$C_{14}H_{11}BrN_4S$	347	537	White solid	0.89	Water	62.19	342	3-(5-(4-bromobenzylthio)-4*H*-1,2,4-triazol-3-yl)pyridine
3g	3-Br	$C_{14}H_{11}BrN_4S$	347	237	Brown solid	0.90	Water	70.39	341	3-(5-(3-bromobenzylthio)-4*H*-1,2,4-triazol-3-yl)pyridine
3h	2-Br	$C_{14}H_{11}BrN_4S$	347	237	Yellow solid	0.90	DMF	59.90	342	3-(5-(2-bromobenzylthio)-4*H*-1,2,4-triazol-3-yl)pyridine
3i	2,4-$(Br)_2$	$C_{14}H_{10}Br_2N_4S$	426	310	Dark brown	0.96	Ethanol	63.73	361	3-(5-(2,4-dibromobenzylthio)-4*H*-1,2,4-triazol-3-yl)pyridine
3j	3,5-$(Br)_2$	$C_{14}H_{10}Br_2N_4S$	426	310	Pale yellow solid	0.95	Ethanol	76.89	362	3-(5-(3,5-dibromobenzylthio)-4*H*-1,2,4-triazol-3-yl)pyridine
3k	4-F	$C_{14}H_{11}FN_4S$	286	178	Yellow solid	0.63	Ethanol	87.25	340	3-(5-(4-fluorobenzylthio)-4*H*-1,2,4-triazol-3-yl)pyridine
3l	3-F	$C_{14}H_{11}FN_4S$	286	178	Red-orange solid	0.63	DMF	78.94	340	3-(5-(3-fluorobenzylthio)-4*H*-1,2,4-triazol-3-yl)pyridine
3m	2-F	$C_{14}H_{11}FN_4S$	286	178	Yellow solid	0.63	Ethanol	75.90	340	3-(5-(2-fluorobenzylthio)-4*H*-1,2,4-triazol-3-yl)pyridine
3n	2,4-$(F)_2$	$C_{14}H_{10}F_2N_4S$	304	311	Yellow brown solid	0.78	Ethanol	89.35	354	3-(5-(2,4-difluorobenzylthio)-4*H*-1,2,4-triazol-3-yl)pyridine

Formation of different 3-(5-(substituted-benzylthio)-4*H*-1,2,4-triazol-3-yl)pyridine derivatives was established by recording there IR, ^{1}H NMR, and MS.

Infrared spectrum of one 1,2,4-triazole derivative 3-(5-(4-chlorobenzylthio)-4*H*-1,2,4-triazol-3-yl)pyridine showed strong C=N stretching (str) band at 1595.76 cm^{-1} and C—N absorption band at 1252.41 cm^{-1} that indicate ring closure of 1,2,4-triazole ring. An absorption band at 2978.85 cm^{-1} is due to aromatic (Ar) C-H str, band at 1630.41 cm^{-1} is due to C=C str, a band at 735.83 cm^{-1} is due to C—Cl str, and band at 657.11 cm^{-1} is due to C—S str. Strong absorption at around 3078.85 and around 1620.47 cm^{-1} was present in all final derivatives, which was confirmed for aromatic C—H and C=C bonds, respectively. The presence of specific functional groups in final synthesized derivatives was confirmed by ^{1}H NMR data. The ^{1}H NMR spectrum of triazole derivatives 3-(5-(4-chlorobenzylthio)-4*H*-1,2,4-triazol-3-

Table 6

Combustion analysis of synthesized 1,2,4-triazole derivatives.

Compounds	Combustion analysis	
	Theoretical value	Observed values
3a	C (55.53%) H (3.66%) Cl (11.7%) N (18.50) S (10.59%)	C (54.53%) H (3.60%) Cl (11.5%) N (18.21) S (10.49%)
3b	C (49.86%) H (2.99%) Cl (21.03%) N (16.61%) S (9.51%)	C (49.26%) H (2.91%) Cl (20.82%) N (16.27%) S (9.41%)
3c	C (55.53%) H (3.66%) Cl (11.7%) N (18.50) S (10.59%)	C (54.55%) H (3.60%) Cl (11.38%) N (18.10) S (10.41%)
3d	C (55.53%) H (3.66%) Cl (11.7%) N (18.50) S (10.59%)	C (55.01%) H (3.59%) Cl (11.38%) N (18.36) S (10.39%)
3e	C (49.86%) H (2.99%) Cl (21.03%) N (16.61%) S (9.51%)	C (49.06%) H (2.94%) Cl (21.0%) N (16.41%) S (9.41%)
3f	C (48.43%) H (3.19%) Cl (23.01%) N (16.14%) S (9.23%)	C (48.02%) H (3.16%) Cl (22.91%) N (16.04%) S (9.20%)
3g	C (48.43%) H (3.19%) Cl (23.01%) N (16.14%) S (9.23%)	C (48.02%) H (3.16%) Cl (22.91%) N (16.04%) S (9.20%)
3h	C (48.43%) H (3.19%) Cl (23.01%) N (16.14%) S (9.23%)	C (48.02%) H (3.16%) Cl (22.91%) N (16.04%) S (9.20%)
3i	C (39.46%) H (2.37%) Br (37.50%) N (13.15%) S (7.52%)	C (39.26%) H (2.32%) Br (37.40%) N (13.11%) S (7.50%)
3j	C (39.46%) H (2.37%) Br (37.50%) N (13.15%) S (7.52%)	C (39.26%) H (2.32%) Br (37.40%) N (13.11%) S (7.50%)
3k	C (58.73%) H (3.87%) F (6.64%) N (19.57%) S (11.20%)	C (57.79%) H (3.85%) F (6.60%) N (19.47%) S (11.12%)
3l	C (58.73%) H (3.87%) F (6.64%) N (19.57%) S (11.20%)	C (57.79%) H (3.85%) F (6.60%) N (19.47%) S (11.12%)
3m	C (58.73%) H (3.87%) F (6.64%) N (19.57%) S (11.20%)	C (57.79%) H (3.85%) F (6.60%) N (19.47%) S (11.12%)
3n	C (55.25%) H (3.31%) F (12.49%) N (18.41%) S (10.54%)	C (54.35%) H (3.30%) F (12.45%) N (18.35%) S (10.50%)

Table 7

Spectral data of synthesized 1,2,4-triazole derivatives.

Compounds	IR (KBr cm^{-1})	^{1}H NMR δ (ppm) (DMSO-d_6)	^{13}C NMR (DMSO-d6, 100 MHz) δ (ppm)	MS
3a	2978.85 (Ar—C—H str), 1630.41 (Ar—C=C str), 1154.87 (Ar—C—C str), 1595.76 (C=Nstr), 1252.41 (—C—N-str), 657.11 (—C—S str), 735. 83 (C—Cl str)	6.84–7.19 (m 4H, Ar—H), 4.25 (s 2H, —CH_2), 7.40–8.90 (m 4H, pyridine ring)	160.7, 154.2, 141.1, 140.0, 138.1, 135.1, 133.0, 130.7, 129.2, 127.9, 122.0, 36.2	301^+
3b	3088.25 (Ar—C—H str), 1610.41 (Ar—C=C str), 1173.78 (Ar—C—C str), 1542.56 (C=Nstr), 1200.41 (—C—N-str), 647.12 (—C—S str), 717.33 (C—Cl str)	6.88–7.29 (m 4H, Ar—H), 4.19 (s 2H, —CH_2), 7.44–8.86 (m 4H, pyridine ring)	156.2, 154.3, 150.2, 146.0, 140.2, 136.1, 135.4, 133.8, 131.3, 128.0, 125.3, 122.0, 37.9	336^+
3c	3108.64 (Ar—C—H str), 1684.40 (Ar—C=C str), 1112.08 (Ar—C—C str), 1521.24 (C=Nstr), 1221.56 (—C—N—str), 612.41.11 (—C—S str), 712.98 (C—Cl str)	6.94–7.46 (m 4H, Ar—H), 4.21 (s 2H, —CH_2), 7.74–8.78 (m 4H, pyridine ring)	159.8, 156.2, 150.1, 147.0, 141.9, 135.3, 134.3, 132.0, 131.2, 129.6, 126.3, 124.9, 122.0, 37.3	301^+
3d	2968.46 (Ar—C—H str), 1598.35.47 (Ar—C=C str), 1175.47 (Ar—C—C str), 1500.36 (C=Nstr), 1285.47 (—C—N-str), 611.81 (—C—S str), 765.79 (C—Cl str)	7.02–7.27 (m 4H, Ar—H), 4.20 (s 2H, —CH_2), 7.63–8.63 (m 4H, pyridine ring)	161.8, 159.5, 149.6, 145.0, 138.1, 135.3, 134.1, 131.0, 129.2, 129.9, 127.6, 126.2, 124.9, 33.1	301^+
3e	2912.56 (Ar—C—H str), 1623.56 (Ar—C=C str), 1121.67 (Ar—C—C str), 1521.12 (C=Nstr), 1213.87 (—C—N-str), 641.78 (—C—S str), 735.13 (C—Cl str)	6.64–7.10 (m 3H, Ar—H), 4.12 (s 1H, —CH_2), 7.30–8.86 (m 4H, pyridine ring)	159.2, 156.9, 149.5, 148.2, 134.1, 133.8, 132.0, 131.2, 130.2, 130.9, 126.0, 123.0, 32.1	336^+
3f	2890.45 (Ar—C—H str), 1611.76 (Ar—C=C str), 1108.45 (Ar—C—C str), 1541.10 (C=Nstr), 1286.45 (—C—N-str), 698.34 (—C—S str), 812.12 (C—Br str)	6.94–7.30 (m 4H, Ar—H), 4.15 (s 2H, —CH_2), 7.60–8.86 (m 4H, pyridine ring)	162.8, 159.5, 150.1, 147.0, 139.7, 135.1, 133.0, 131.6, 129.0, 125.0, 123.5, 36.2	346^+
3g	3134.78 (Ar—C—H str), 1652.89 (Ar—C=C str), 1146.89 (Ar—C—C str), 1511.21 (C=Nstr), 1264.76 (—C—N-str), 698.98 (—C—S str), 842.45 (C—Br str)	7.10–7.30 (m 4H, Ar—H), 4.19 (s 2H, —CH_2), 7.44–8.84 (m 4H, pyridine ring)	159.8, 156.5, 149.1, 144.0, 140.9, 136.1, 134.0, 132.2, 131.7, 130.1, 127.8, 125.0, 122.1, 34.5	346^+
3h	3078.45 (Ar—C—H str), 1662.67 (Ar—C=C str), 1109.78 (Ar—C—C str), 1500.90 (C=Nstr), 1210.43 (—C—N-str), 690.56 (—C—S str), 832.56 (C—Br str)	6.96–7.31 (m 4H, Ar—H), 4.19 (s 2H, —CH_2), 7.44–8.81 (m 4H, pyridine ring)	161.3, 158.3, 152.1, 148.0, 138.2, 137.1, 134.0, 131.7, 129.0, 128.4, 126.8, 123.0, 121.7, 32.4	346^+
3i	2910.56 (Ar—C—H str), 1623.56 (Ar—C=C str), 1101.67 (Ar—C—C str), 1561.12 (C=Nstr), 1210.87 (—C—N-str), 691.78 (—C—S str), 842.12 (C—Br str)	6.86–7.41 (m 3H, Ar—H), 4.19 (s 2H, —CH_2), 7.42–8.88 (m 4H, pyridine ring)	160.8, 156.5, 151.1, 149.0, 139.8, 138.2, 136.1, 135.0, 131.2, 130.2, 125.9, 124.0, 122.7, 31.4	425^+

(*Continues*)

Table 7

(*Continued*)

Compounds	IR (KBr cm^{-1})	^{1}H NMR δ (ppm) (DMSO-d_6)	^{13}C NMR (DMSO-d6, 100 MHz) δ (ppm)	MS
3j	2922.12 (Ar—C—H str), 1615.45 (Ar—C═C str), 1135.60 (Ar—C—C str), 1515.10 (C═Nstr), 1235.10 (—C—N-str), 690.80 (—C—S str), 820.90 (C—Br str)	7.10–7.41 (m 3H, Ar—H), 4.18 (s 2H, $-CH_2$), 7.43–8.87 (m 4H, pyridine ring)	158.2, 156.5, 149.7, 14890, 143.1, 135.1, 132.2, 131.0, 130.5, 125.3, 124.0, 35.4	425^{+}
3k	3113.20 (Ar—C—H str), 1590.45 (Ar—C═C str), 1130.60 (Ar—C—C str), 1492.10 (C═Nstr), 1230.10 (—C—N-str), 703.89 (—C—S str), 1370.90 (C—F str)	6.98–7.25 (m 4H, Ar—H), 4.19 (s 2H, $-CH_2$), 7.44–8.84 (m 4H, pyridine ring)	162.3, 158.2, 157.1, 150.1, 148.7, 138.3, 136.1, 134.0, 128.4, 124.8, 118.5, 38.0	285^{+}
3l	3087.89 (Ar—C—H str), 1657.89 (Ar—C═C str), 1147.78 (Ar—C—C str), 1547.89 (C═Nstr), 1290.56 (—C—N-str), 725.78 (—C—S str), 1400.89 (C—F str)	7.10–7.30 (m 4H, Ar—H), 4.22 (s 2H, $-CH_2$), 7.50–8.90 (m 4H, pyridine ring)	162.2, 159.8, 157.8, 149.6, 148.0, 143.3, 137.1, 133.0, 131.4, 126.0, 125.4, 115.8, 111.9, 39.2	285^{+}
3m	3089.56 (Ar—C—H str), 1634.56 (Ar—C═C str), 1111.89 (Ar—C—C str), 1543.87 (C═Nstr), 1233.89 (—C—N-str), 612.87 (—C—S str), 1321.89 (C—F str)	7.08–7.28 (m 4H, Ar—H), 4.17 (s 2H, $-CH_2$), 7.48–8.82 (m 4H, pyridine ring)	161.3, 159.8, 155.5, 149.1, 147.0, 138.1, 135.0, 130.4, 128.8, 127.1, 122.4, 115.9, 33.0	285^{+}
3n	3099.90 (Ar—C—H str), 1555.12 (Ar—C═C str), 1172.98 (Ar—C—C str), 1496.89 (C═Nstr), 1298.67 (—C—N-str), 695.90 (—C—S str), 1380.90 (C—F str)	6.76–7.31 (m 3H, Ar—H), 4.15 (s 2H, $-CH_2$), 7.60–8.62 (m 4H, pyridine ring)	162.2, 161.6, 159.8, 154.5, 149.1, 144.0, 134.1, 132.0, 131.0, 125.0, 123.7, 110.1, 134.7, 29.4	303^{+}

yl)pyridine shown in the region 6.84–7.19 is due to four aromatic proton, 7.40–8.90 is due to four pyridine proton, and 4.25 is due to two methylene proton. The presence of another group like $-CH_3$ synthesized derivatives was confirmed by shift value 3.67. The mass spectra of triazole derivative 3-(5-(4-chlorobenzylthio)-4*H*-1,2,4-triazol-3-yl)pyridine showed a molecular ion peak at *m/z* 301^{+}, which is in conformity with the molecular formula $C_{14}H_{11}ClN_4S$. In the same way, spectral data of remaining derivatives are given in Table 7.

Table 8

Antimicrobial activity of synthesized 1,2,4-triazole derivatives using plate hole diffusion method (10 mg/mL).

	Zone of inhibition (mm)							
	Antibacterial activity						Antifungal activity	
	Gram-negative bacteria			Gram-positive bacteria				
Compounds	*Escherichia coli*	*Pseudomonas aeruginosa*	*Acinetbacter baumannii*	*Staphylococcus aureus*	*Streptococcus pyogenes*	*Enterococcus faecalis*	*Aspergillus clavatus*	*Candida albicans*
3a	11	11	8	10	09	–	–	7
3b	11	10	6	10	09	–	–	5.5
3c	11	12	9	08	08	7	–	–
3d	12	11	10	11	12	5.5	6	
3e	12	08	5.5	11	10	5.5	–	–
3f	12	12	–	12	13	8	–	5.5
3g	11	11	5.5	10	11	6	–	–
3h	13	13	8	12	13	8	8	–
3i	13	12	9	13	12	6	–	8
3j	12	11	7	12	11	7	–	–
3k	11	10	8	10	09	8	5.5	–
3l	12	11	–	11	11	5.5	6	–
3m	11	11	6	11	12	6	–	6
3n	08	11	5.5	09	09	–	–	–
DMSO	–	–	–	–	–	–	–	–
Mithotrixate	14	13	12	13	14	10	–	–
Fluconazole	–	–	–	–	–	–	11	12

#Diameter of zone of inhibition expressed in mm.

Further, we have screened the antibacterial activity of newly synthesized 1,2,4-triazole derivatives. The tested derivatives exhibited 5.5–13 mm zone of inhibition in 10 mg/mL concentration against Gram-negative bacteria and Gram-positive bacteria, whereas standard drug methotrexate showed 10–14 mm zone of inhibition. The synthesized compounds were shown very weak antifungal activity. (Table 8).

The minimal inhibitory concentration study was performed on synthesized compounds. The results were shown in Table 9.

Out of all synthesized derivatives, two derivatives, that is, 3-(5-(2-bromobenzylthio)-4*H*-1,2,4-triazol-3-yl)pyridine and 3-(5-(2,4-dibromobenzylthio)-4*H*-1,2,4-triazol-3-yl)pyridine showing more potent antibacterial activity (Fig. 2). Triazole nucleus containing compounds has revealed nice-looking pharmacological activity. It may note that the 3-position and 5-position of triazole nucleus are extremely important sites for molecular modification, which can play a dominant role in determining the pharmacological activities of triazole derivatives. Therefore, we have attempted to develop the derivatives of triazole nucleus at 3-position and 5-position with a view to evaluating further the potency of the molecules. In the present study, as discussed earlier, we have modified the 1,2,4-triazole derivatives linked substituted benzyl groups via thio linkage. The resulting compounds produced 80–90% efficacy as compared with standard against Gram-negative, Gram-positive bacteria. Results revealed that novel 1,2,4-triazole-linked with substituted benzyl groups via thio linkage showed significant antibacterial activities as compared with standard drug methotrexate.

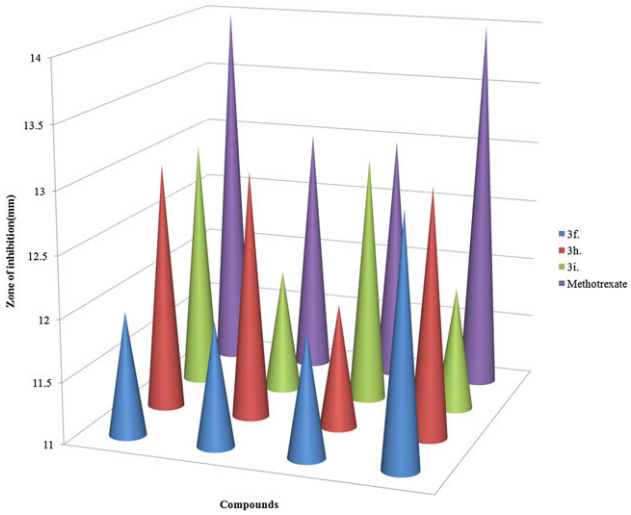

Figure 2. Comparative antibacterial evaluation of compound **3f**, **3h**, and **3i** with respect to methotrexate. [Color figure can be viewed at wileyonlinelibrary.com]

DOCKING STUDY

To rationalize the potency of the molecules as an antimicrobial agent, these compounds were docked against DHFR from *E. coli* and *Lactobacillus* (4DFR) obtained from protein data bank (RCSB). The binding

Table 9

Antimicrobial activity of the synthesized compounds expressed as MIC (mg/mL).

	MIC (mg/mL)							
	Antibacterial activity						Antifungal activity	
	Gram-negative bacteria			Gram-positive bacteria				
Compounds	*Escherichia coli*	*Pseudomonas aeruginosa*	*Acinetbacter baumannii*	*Staphylococcus aureus*	*Streptococcus pyogenes*	*Enterococcus faecalis*	*Aspergillus clavatus*	*Candida albicans*
3a	1.57	2.03	3.97	2.15	4	15	11	7.5
3b	1.78	2.01	5.96	2.8	3.9	16.7	23.5	9.2
3c	1.83	1.73	3.02	4	4.75	6.9	22.1	23.4
3d	1.29	1.97	2.86	2.1	1.1	7.1	6.9	12.5
3e	1.1	3.89	6.96	2.1	2.1	8.5	21.0	24.5
3f	1.21	1.33	13.03	1.15	0.95	3.75	12.1	8.9
3g	1.74	1.98	6.09	2.75	1.75	9	23.0	12.8
3h	0.98	0.91	3.84	1.2	0.98	3.9	4.2	11.5
3i	0.99	1.21	3.10	1	1.2	8.5	24.1	3.8
3j	1.23	1.98	3.08	1.3	1.9	3.8	22.5	24.5
3k	1.86	2.12	3.8	2.2	3.5	3.2	8.2	23.6
3l	1.17	2	15.3	1.9	2.15	9.5	8.4	23.2
3m	2.1	1.98	3.9	1.95	1.25	8.6	23.1	8.6
3n	3.01	2.01	6.1	2.9	3.2	12	22.8	22.5
DMSO	–	–	–	–	–	–	–	–
Mithotrixate	0.8	0.82	0.95	0.96	0.8	1.25	NT	NT
Fluconazole	NT	NT	NT	NT	NT	NT	1.10	1.20

MIC, minimal inhibitory concentration; NT, not tested.

energy of drug-receptor complex and standard drug is shown in Table 4.

All synthesized molecules interacted with the active sites of DHFR enzyme (4DFR) through various bonds like hydrogen, van der Waals, p-cation, p-anion, p-alkyl, p-donor hydrogen, p-sulfur, carbon-hydrogen bond, and p-sigma. As shown in Table 6, binding energies of the molecules against the active sites indicated a higher affinity of the molecules to bind to the protein leading to the inhibition. The binding energies of the molecules ranging from −10.5369 to −11.8477 kcal/mol and were better as compared with standard drug methotrexate. The nitrogen atoms of the pyridine and triazole ring of synthesized compounds are responsible for the form hydrogen bond with the different amino acid of a receptor (Table 6). Out of 16 amino acid residue of DHFR that is responsible for the formation of bonds with methotrexate, 8 to 10 were found to be similar in compounds **3d**, **3f**, **3g**, **3h**, **3i**, **3l**, and **3m**. The synthesized compounds active site alignment showed a pattern resemblance to the binding pocket alignment of methotrexate (Fig. 3). According to docking study results, the difference in biological activity of tested compounds despite their similar chemical structure could be explained on the basis of its alignment with receptor binding pocket as well as interaction with particular amino acid residue. The

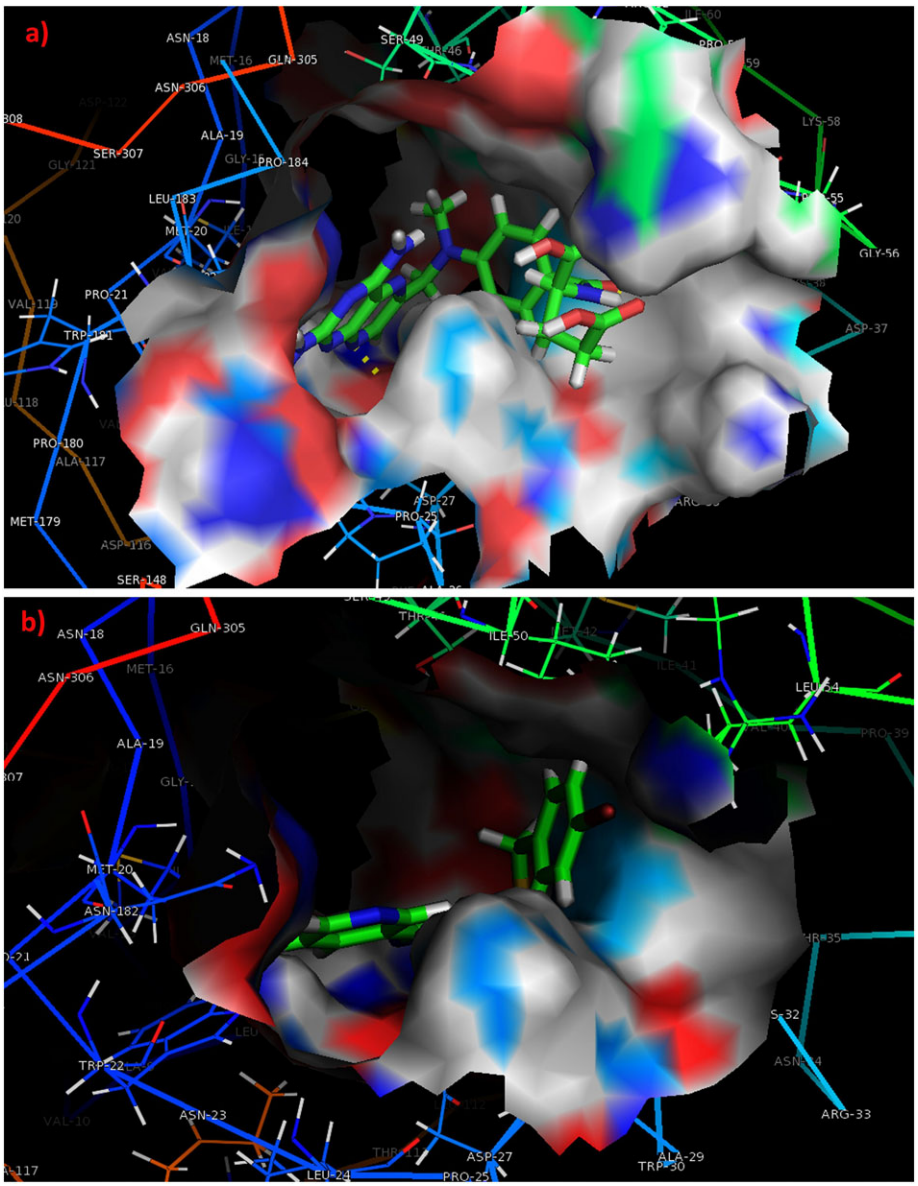

Figure 3. Interaction of compound **3f** and methotrexate with the binding domain of the dihydrofolate reductase enzyme (4DFR). [Color figure can be viewed at wileyonlinelibrary.com]

compound **3f** showed antibacterial activity near about to that **3h** and **3i**, instated of having low docking score compared with **3h** and **3i**. This is due to the higher resemblance to binding pocket alignment (10 amino acid residue) of methotrexate.

CONCLUSION

A new series of different 3-(5-(substituted-benzylthio)-4*H*-1,2,4-triazol-3-yl)pyridine derivatives were prepared by treating 5-mercapto-3-pyridyl-1,2,4-triazole with differently substituted benzyl halides, by a simple, suitable, and well-organized synthetic route. Physical and analytical parameters of the newly synthesized 1,2,4-triazole derivatives were confirmed by TLC, IR, NMR, and MS. Subsequently, in antimicrobial screening, the compounds showed antimicrobial activity. In antimicrobial screening, 3-(5-(2-bromobenzylthio)-4*H*-1,2,4-triazol-3-yl) pyridine and 3-(5-(2,4-dibromobenzylthio)-4*H*-1,2,4-triazol-3-yl)pyridine showing more potent antibacterial activity as compare with other derivatives. The results of docking studies also conform the mechanism of antimicrobial action, that is, by inhibition of DHFR enzyme. Thus, we concluded that the data of the present study may pave a way for the development of novel antibacterial agents with good efficacy and lesser adverse effects. Moreover, results of docking study enforce us for anticancer evaluation of synthesized molecules in future due to its higher binding affinity to DHFR than methotrexate.

Acknowledgments. The authors thank to the Management of School of Pharmacy, Chouksey Engineering College, Bilaspur, for providing necessary infrastructural facilities, and RGPV, Bhopal, for providing immense help in the spectral analysis.

REFERENCES AND NOTES

[1] Chen, Q.; Zhu, X. L.; Jiang, L. L.; Liu, Z. M.; Yang, G. F. Eur J Med Chem 2008, 43, 595.

[2] Bayrak, H.; Demirbas, A.; Demirbas, N.; Karaoglu, S. A. M. Eur J Med Chem 2010, 45, 4726.

[3] Agarwal, N.; Kumar, R.; Dureja, P.; Khurana, J. M. Eur J Med Chem 2011, 46, 4089.

[4] Sharma, S.; Saquib, M.; Verma, S.; Mishra, N. N.; Shukla, P. K. Eur J Med Chem 2014, 83, 474.

[5] Klimesova, V.; Zahajska, L.; Waisser, K.; Kaustova, J.; Mollmann, U. Farmacoterapia 2014, 59, 79.

[6] Mali, R. K.; Somani, R. R.; Toraskar, M. P.; Mali, K. K.; Naik, P. P.; Shirodkar, P. Y. Int J Chem Tech Res 2009, 1, 168.

[7] Kucukguzel, I.; Kucukguzel, S. G.; Rollas, S.; Kiraz, M. Med Chem Lett 2001, 11, 1703.

[8] Al-Omar, M. A.; Al-Abdullah, E. S.; Shehata, I. A.; Habib, E. E.; Ibrahim, T. M.; El-Emam, A. A. Molecules 2010, 15, 2526.

[9] Mathew, V.; Keshavayya, J.; Vaidya, V. P.; Giles, D. Eur J Med Chem 2007, 42, 823.

[10] Amir, M.; Kumar, S. Acta Pharm 2007, 57, 31.

[11] Tozkoparan, B.; Gokhan, N.; Aktay, G.; Yesilada, E.; Ertan, M. Eur J Med Chem 2007, 35, 743.

[12] Tozkoparan, B.; Kupeli, E.; Yesilada, E.; Ertan, M. Bioorganic Med Chem Lett 2007, 15, 1808.

[13] Mhasalkar, M. Y.; Shah, M. H.; Nikam, S. T.; Ananthanarayana, K. G.; Deliwala, C. V J of Med Chem 1970, 13, 672.

[14] Przegalinski, E.; Lewandowska, A. J Neural Transm 1979, 46, 303.

[15] Langley, M. S.; Clissold, S. P.; Brotizolam Drugs 1988, 35, 104.

[16] Kelley, J. L.; Koble, C. S.; Davis, R. G.; McLean, E. W.; Soroko, F. E.; Cooper, B. R. J Med Chem 1995, 38, 4131.

[17] Kumar, D.; Kumar, N. M.; Chang, K. H.; Shah, K. Eur J Med Chem 2010, 45, 4664.

[18] El-Nassan, H. B. Eur J Med Chem 2011, 46, 2031.

[19] El Sayed Aly, M. R.; Saad, H. A.; Mohamed, M. A. M. Med Chem Lett 2015, 25, 2824.

[20] Hassan, G. S.; El-Messery, S. M.; Al-Omary, F. A.; Shabayek, M. I.; Abulfadl, Y. S.; Habib, e.-S. E.; El-Hallouty, S. M.; Fayad, W.; Mohamed, K. M.; El-Menshawi, B. S.; El-Subbagh, H. I. Eur J Med Chem 2013, 66, 135.

[21] El-Gazzar, Y. I.; Georgey, H. H.; El-Messery, S. M.; Ewida, H. A.; Hassan, G. S.; Raafat, M. M.; Ewida, M. A.; El-Subbagh, H. I. Bioorg Chem 2017, 72, 282.

[22] Paliwal, S.; Sharma, S.; Dwivedi, J.; Mishra, A. J Het Chem 2017, 54, 3689.

[23] Dewangan, D.; Pandey, A.; Sivakumar, T.; Rajavel, R.; Dubey, R. Int J ChemTech Res 2010, 2, 1397.

[24] Dewangan, D.; Tripathi, D. K.; Verma, T.; Nagori, K.; Shah, V.; Rajawel, R. Int J ChemTech Res 2011, 3, 948.

[25] Badwaik, H.; Vekatraman, S.; Thakur, D.; Vinod, M.; Raamamurthy, J.; Dshmukh, K. Asian J Res Chem 2011, 4, 893.

[26] Rajput, S.; Sisodia, D.; Badwaik, H.; Thakur, D.; Nagori, K. Asian J Res Chem 2011, 4, 40.

[27] Badwaik, H.; Sonkar, S.; Singh, M.; Rajput, S.; Sisodiya, D.; Pandey, A. Asian J Res Chem 2009, 2, 544.

[28] Hassan, F.; Kamal, A.; Ahmad, N.; Nasibullah, M.; Khan, M. S.; Khan, A. R. Int J Chem 2014, 34, 1395.

[29] Liszkiewicz, H.; Kowalska, M. W.; Wietrzyk, J.; Opolski, A. Indian J Chem 2003, 42B, 2846.

[30] Ahirwar, J.; Ahirwar, D.; Lanjhiyana, S.; Jha, A. K.; Dewangan, D.; Badwaik, H. J Het Chem 2018. https://doi.org/10.1002/jhet.3258.

SUPPORTING INFORMATION

Additional supporting information may be found online in the Supporting Information section at the end of the article.